Investigation of Molecular Weight and Aging Effects on the Stiffness of Polyelectrolyte Multilayer Microcapsules

ARTICLE *in* MACROMOLECULES · SEPTEMBER 2004

Impact Factor: 5.8 · DOI: 10.1021/ma049140+

3 AUTHORS, INCLUDING:

Olga I Vinogradova
Russian Academy of Sciences
111 PUBLICATIONS **3,382** CITATIONS

Investigation of Molecular Weight and Aging Effects on the Stiffness of Polyelectrolyte Multilayer Microcapsules

Valentin V. Lulevich,[†,‡] Simon Nordschild,[†] and Olga I. Vinogradova*[,†,‡]

Max Planck Institute for Polymer Research, Ackermannweg 10, 55128 Mainz, Germany, and Laboratory of Physical Chemistry of Modified Surfaces, Institute of Physical Chemistry, Russian Academy of Sciences, 31 Leninsky Prospect, 119991 Moscow, Russia

Received May 3, 2004; Revised Manuscript Received July 23, 2004

ABSTRACT: By using a combination of atomic force and confocal microscopy, we explore the effect of molecular weight and aging on the mechanical properties of polyelectrolyte multilayer microcapsules. Within the variability of experimental data, the force vs relative deformation curves and images from confocal scanning of the deformed capsules were found to be the same for all molecular weights used. The freshly prepared polyelectrolyte microcapsules were found to be stiffer than the aged ones. This time softening or aging was shown to be due to faster drainage of the inner solution. Such a rapid drainage is probably caused by an enhanced fragility (or a decrease in the rupture strength) of the multilayer and is observed despite a detected reduction of nanopore size and number. These results are consistent with the concept of a rubbery (elastomeric) state of the multilayer.

Introduction

Recently, there has been much interest in studying polyelectrolyte multilayer microcapsules.[1] Being potentially important for a variety of applications, these microcapsules represent a convenient system for investigating physical properties of free-standing polyelectrolyte multilayer films forming their shells. For example, by studying deformation behavior of microcapsules in various conditions, one can deduce an inference about such properties of the shell material as permeability, elasticity, rupture strength, and more (for a recent review see ref 2).

We have recently suggested two novel quantitative approaches to probe the mechanical properties of the polyelectrolyte multilayers forming the capsule shell. One method is based on studying the swelling of microcapsules filled with a solution of strong polyelectrolyte.[3] Another approach, motivated by earlier studies,[4,5] involves measuring the deformation of microcapsules under applied load using atomic force microscopy (AFM).[6] Both methods have given, for multilayers assembled initially on melamine formaldehyde (MF) particles, a value of Young's modulus of the order of 100−200 MPa. This falls in the range characteristic for elastomers.[7] A typical mechanical behavior for elastomers reflects strong interactions between polyanions and polycations in the multilayer and indicates that we are dealing with a physically cross-linked network structure. Indeed, the high number of ionic pairs present in the multilayers[8,9] might serve as the cross-linking units of such a network.

Several important consequences follow from the rubbery (elastomeric) state of polyelectrolyte multilayers[3,6] and its possible interpretation in terms of ionic cross-linking.[10,11] First, this immediately indicates that pH and salt should be important parameters to regulate the charge density, number of cross-linking units, and the strength of ionic bonding. Indeed, our recent study has proven that Young's modulus of the multilayer depends strongly on the charge density of shell-forming polymers and that this can be changed by variation of pH and salt.[10,11] Second, since the properties of elastomer materials are mostly controlled by the number of (in our case, ionic) cross-links, the polymer molecular weight should be a variable of much lesser importance. In other words, one can expect there to be only a minor influence of chain length on the multilayer mechanics. Third, since the multilayer films show long-term stability in various solutions while not in thermodynamic equilibrium,[9,12] one can speculate that such a stability can be attributed to the same type of physical (ionic) cross-linking as responsible for elastomer-like mechanical behavior.[10] Then the cross-links reduce the mobility of the polyelectrolyte chains, thus freezing the structure of the multilayer. If so, one can expect some possible rearrangement of molecular fragments on a relatively large time scale, which could lead to some changes in structure and mechanical properties of the multilayer shells.

There has been, however, another quantitative approach to probe the elasticity of shell-forming multilayers, based on observing osmotically induced buckling of microcapsules immersed in polyelectrolyte solution.[13] The values of Young's modulus (for multilayers assembled on MF particles) obtained with this method is of the order of 1000−1500 MPa. This led to the conclusion that polyelectrolyte multilayers represent quite a rigid material, comparable to a bulk plastic.[7] In such a case one can expect some dependence of mechanical properties on molecular weight of shell-forming polyelectrolytes. In contrast, a time evolution of the structure and properties (elasticity, permeability) should hardly be expected, taking into account that the interaction between polyelectrolytes forming a plastic material should be extremely strong.

Thus, Young's modulus obtained in the AFM and osmotic swelling experiments is an order of magnitude lower than that obtained in an osmotic buckling experiment on the same type (MF) of capsules. An order of magnitude difference cannot be treated as large, taking

† Max Planck Institute for Polymer Research.
‡ Russian Academy of Sciences.
* Corresponding author: e-mail vinograd@mpip-mainz.mpg.de.

10.1021/ma049140+ CCC: $27.50
Published on Web 09/10/2004

into account the accuracy of experimental data, assumptions of theoretical models, and the sensitivity of the multilayer shells to the preliminary treatment and/or preparation conditions.[2] Therefore, at the moment it is difficult to draw more definite conclusions about the Young's modulus value. However, since the consequences of such differences concern mostly the physical state of the multilayer, it follows from the above that one can try to obtain data in favor of one (elastomer) or another (bulk plastic) points of view by investigating the influence on mechanical properties of such factors as molecular weight and aging.

The effect of molecular weight of the polyelectrolytes on the multilayer structure and properties has been explored before. Observed effects on the assembly, structure, and thickness of supported multilayer films were extremely small.[9,8,14−17] The weak influence on the structure of obtained film suggests similarities in mechanical properties, although it does not of course entirely exclude possible differences. However, little is known so far about possible changes in the multilayer stiffness with molecular weight. To our knowledge, there has been only one attempt to estimate the effect of molecular weight on the multilayer elasticity, made with an osmotic buckling technique,[13] which suggested that Young's modulus of the multilayer slightly increases with molecular weight of a polycation. The dependence on molecular weight found in ref 13 is more consistent with the behavior of bulk plastic materials than that of rubbers. However, these preliminary conclusions are based on limited experimental data (molecular weight of a polyanion was fixed, and only two molecular weights of a rather polydisperse polycation, M_w 8−15 and 50−65 kDa, were taken) and seem to be in apparent disagreement with the structure studies.[9,8,14,15]

To our knowledge, the question of aging, i.e., of possible time evolution of structure and properties (elasticity, permeability, etc.) of the multilayer shells, has been never addressed before. Multilayer microcapsules are known to show remarkable long-term stability, but only in the sense that they keep their shape and size.[2] There have been several studies of the conformational relaxations during adsorption, but they concerned mostly the short time scale and reported equilibration after several minutes.[18−21]

In this paper we use the AFM approach in combination with confocal microscopy to explore the effect of molecular weight of shell-forming polyelectrolytes on the stiffness of multilayer microcapsules. As before,[3−5] we study capsules with shells composed of layers of alternating poly(sodium styrene) sulfonate and poly(allylamine) hydrochloride. However, now we vary the molecular weight of both polyanions and polycations over a wide range. Our conclusion is that the force vs deformation profiles and images from confocal scanning are the same for all shells within the accuracy of the experiment. We also extend our earlier work into study of aging properties of multilayer shells and make entirely new observations on the softening of capsules with time. This softening (smaller force at the same deformation) is shown to be due to an increase in the shell permeability under compression and again does not depend on the molecular weights of shell-forming polyelectrolytes. We demonstrate that the enhanced permeability of the multilayer is not due to defects in the shell, which, in contrast, are prone to disappear with time, but rather due to enhanced fragility. Compared with earlier work we have now considerably improved the resolution of optical images of deformed capsules, enabling a characterization of the shape and volume of the capsules and permeability of the multilayer shell during an AFM compression experiment. We also use higher magnification scanning electron microscopy (SEM), which allows us to explore the evolution of the nanopore structure of the shells. Our results strongly support the concept of a rubbery (elastomeric) state of the multilayer.[2,3,6]

Table 1. Molecular Weight (kDa) of Shell-Forming Polyelectrolytes Used in Different Samples

	PSS		PAH	
sample	70	1000	15	70
1	x		x	
2	x			x
3		x	x	
4		x		x

II. Materials and Methods

The capsules were produced in 1 mol/L NaCl (pH 6) according to the method[22] based on LbL assembly of four bilayers of polystyrenesulfonate (PSS, $M_w \sim 70$ and 1000 kDa, Aldrich) and poly(allylamine) hydrochloride (PAH, $M_w \sim 15$ and 70 kDa, Aldrich) layers on weakly cross-linked monodisperse melamine formaldehyde particles (MF) purchased from Microparticles GmbH (Berlin, Germany). The MF particles were of radius 2.0 ± 0.1 μm and were dissolved using HCl (at pH 1.2−1.4). Using polyelectrolytes of these molecular weights, we have prepared four samples of capsules (see Table 1). The capsules studied within 1 month after preparation are referred below as $\mathcal{N}$ (i.e., newly prepared) capsules. The capsules kept in water for more than 6 months after preparation are referred to below as $\mathcal{A}$ (i.e., aged) capsules.

FITC-dextran ($M_w \sim 4$, 70, and 150 kDa) and low molecular weight dye rhodamine for permeability tests were purchased from Aldrich. RBITC−PSS was synthesized according to modifications of the method[23] described in refs 3 and 11.

Load (force) vs deformation curves were measured with the molecular force probe (MFP) 1D AFM (Asylum Co, Santa Barbara, CA) equipped with a nanopositioning sensor that corrects piezoceramic hysteresis and creep. The MFP was used together with a commercial confocal microscope manufactured by Olympus (Japan) consisting of the conconfocal laser scanning unit Olympus FV 300 in combination with an inverted fluorescence microscope Olympus IX70 equipped with a high-resolution bright (NA = 1.45) immersion oil objective (60×). The confocal microscope was specially adapted for the MFP 1D (two micrometric tables, sample lifting device, etc.). This allowed optical measurements of the capsule's shape during the AFM force experiment. The excitation wavelengths were chosen according to the label rhodamine (543 nm) and fluorescein (488 nm). The *z*-position scanning was done in steps of 0.02−0.05 μm. High resolution and contrast of the confocal images were achieved due to use of the fluorescent dye RBITC−PSS at a concentration of 10^{-6} mol/L.

A schematic of the experiment is presented in Figure 1. A drop (50−100 μL) of water (purified by a commercial Milli-Q Gradient A10 system containing ion exchange and charcoal stages) suspension of polyelectrolyte microcapsules was deposited onto a thin glass slide fixed over the oil immersion objective of the confocal microscope. A glass sphere (radius $r_s = 20 \pm 1$ μm, Duke Sci. Co., CA) attached to a cantilever (V-shaped, Micromash, Estonia, spring constant $k = 2.5$ N/m) was centered above the apex of a capsule with accuracy of ± 0.5 μm, using the graticule lines in the optical image for alignment. Measurements were performed at a speed in the range from 0.2 to 20 μm/s.

The result of measurements gives the deflection Δ vs the position of the piezotranslator during a single approach (loading). The load, $\mathcal{F}$, was determined from the cantilever

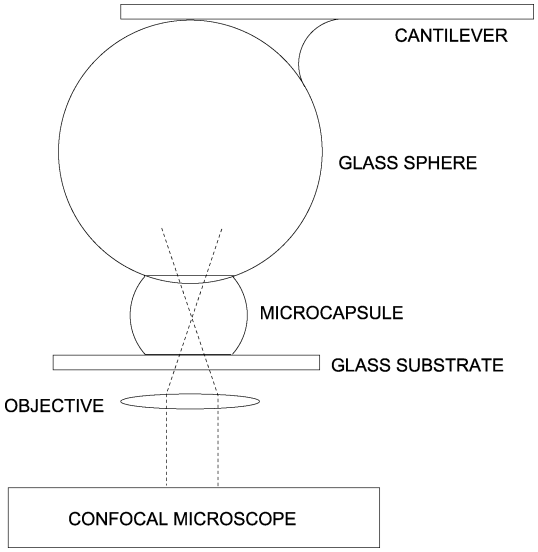

Figure 1. Schematic of the AFM force experiment.

deflection, $\mathcal{F} = k\Delta$. As before, we assume that the zero of separation is at the point of the first measurable force.[4] Then the deformation is calculated as the difference between the position of the piezotranslator and cantilever deflection.

The diameters of the capsules were determined optically with an accuracy of 0.4 μm and from the AFM load vs deformation curves (see ref 4 for more details). The relative deformation ϵ of the capsule was then defined as $\epsilon = 1 - H/(2r_0)$, where r_0 is the radius of the undeformed capsule and H is the distance between glass surfaces.

As was reported before,[4] the capsules reveal some variability in behavior. Therefore, to get reliable results, we have performed several series of (at least 10−20) experiments for each sample. Typically 5−10% of the capsules were too stiff (due to the MF fragments of the initial templates remaining in the shells) or too soft (being broken during the template dissolution process) compared with the average value in the series. In these cases we have not observed the typical (quantitatively) force curves. These data were ignored in our analysis.

For SEM analysis a drop of each sample solution was applied to a silicon wafer with sequential drying at room temperature for 2−3 h. Then measurements were performed using a Gemini Leo (Zeiss) 1530 instrument operating at a working distance of 2 mm and an acceleration voltage of 0.5 kV. Since the samples were not covered with a gold layer before inspection, this low acceleration voltage was applied in order to avoid charging of the sample. The images were recorded using an InLens detector.

III. Results and Discussion

Figure 2 shows load vs deformation profiles typical for $\mathcal{N}$ capsules. The difference between the results obtained for four samples (Table 1) is within the variability between the results obtained for one sample. By analyzing these profiles and confocal images (Figure 2), we have confirmed the conclusions made before.[4,5] Namely, we have observed the elastic regime of deformation at $\epsilon \leq 0.2-0.3$, where the deformation is completely reversible, independent of the driving speed, and the free area of the capsules remains spherical (Figure 2). For all samples for relative deformations $0.2-0.3 \leq \epsilon \leq 0.7-0.8$ we observed only partial reversibility in loading/unloading, noisy regions in the deformation profiles, and significant dependence on the driving speed, which indicates drainage of the inner solution through the shell and/or its local rupture. This is also confirmed by a confocal scan (Figure 2) which shows that the equatorial cross sections of the capsule

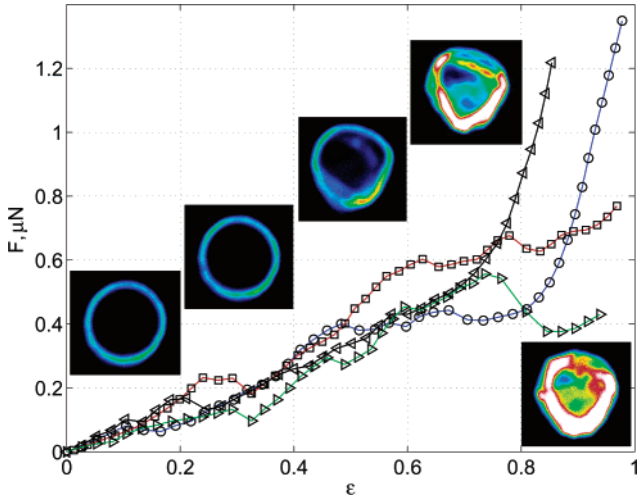

Figure 2. Force vs relative deformation, ϵ, curves for $\mathcal{N}$ capsules. Blue, black, red, and green curves are the profiles for sample 1, 2, 3, and 4, respectively. Driving speed 20 μm/s. Insets show confocal images (equatorial cross section) of deformed capsules at given ϵ. From left to right $\epsilon = 0.1$, 0.3, 0.5, 0.7, and 0.9.

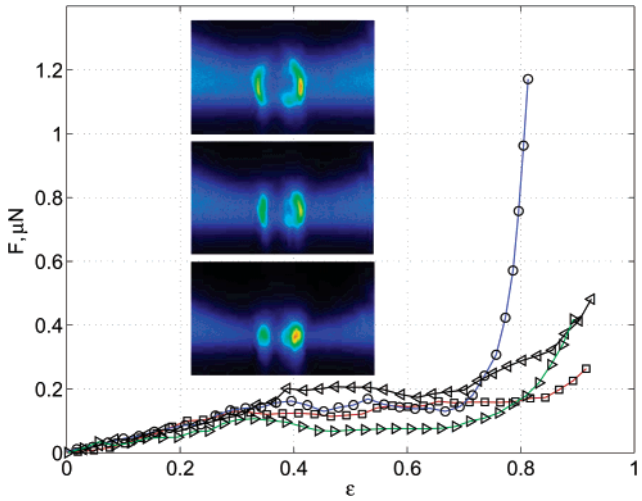

Figure 3. Force vs relative deformation, ϵ, curves for $\mathcal{A}$ capsules. Blue, black, red, and green curves are the profiles for sample 1, 2, 3, and 4, respectively. Driving speed 20 μm/s. Insets show confocal images (z-scanning) of deformed capsules at given ϵ. From top to bottom $\epsilon = 0.3$, 0.5, and 0.7.

shells deviate from a circular shape. A total destruction of the capsules and irreversible deformation were observed at $\epsilon \geq 0.7-0.8$.

By performing the same force and confocal measurements for $\mathcal{A}$ capsules, we have observed the same regimes of reversible, only partially reversible, and completely irreversible deformations, all corresponding to roughly the same ϵ as in the case of $\mathcal{N}$ capsules. However, we found that $\mathcal{A}$ capsules are softer (weaker force at the same ϵ) than $\mathcal{N}$ capsules. Figure 3 shows deformation curves typical for each of four samples. Also included in Figure 3 are the confocal images (z-scanning) measured at different relative deformation. The comparison of measured data presented in Figures 2 and 3 shows even a qualitative difference, especially in the regime of partial reversibility of deformations ($0.2-0.3 \leq \epsilon \leq 0.7-0.8$). Namely, in contrast to $\mathcal{N}$ capsules, which reveal a tendency to become stiffer, the $\mathcal{A}$ capsules show deformation at quasi-constant load. This indicates that drainage of the inner solution become

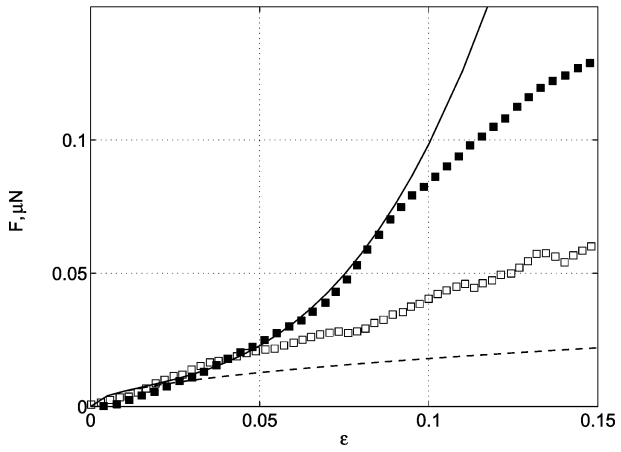

Figure 4. Force vs relative deformation, ϵ, curves. Open symbols correspond to the average profile for $\mathcal{A}$ capsules. Filled symbols plot the average curve for $\mathcal{N}$ capsules. Driving speed 2 μm/s. Fit to eq 1 (solid curve) gives $E = 200$ MPa for $\epsilon \leq 0.1$. The dashed curve shows the force vs deformation profile expected for an infinitely permeable capsule (eq 2) with the same Young's modulus.

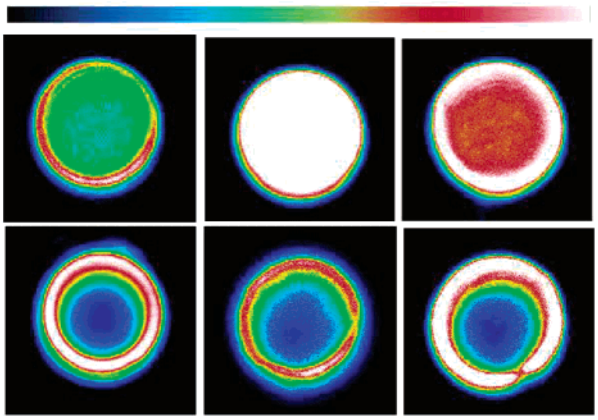

Figure 5. Confocal images (the offset parameter is equal to zero) of $\mathcal{N}$ (top) and $\mathcal{A}$ (bottom) capsules immersed into a solution of FITC-dextran for 24 h. From left to right $M_w \sim 4$, 70, and 150 kDa. Color bar indicates the mapping of intensity of fluorescence value to color: from left to right the intensity changes from 0 to 1 au.

more rapid than for freshly prepared capsules. Again, there is no significant difference between the four samples, so that we do not observe any influence of molecular weight of shell-forming polyelectrolyte on the mechanical properties.

To examine the significance of permeability of compressed capsules more closely and to evaluate Young's modulus of the multilayers, the average small deformation profile for $\mathcal{A}$ capsules is given in Figure 4. For comparison, the average force curve for $\mathcal{N}$ capsules is also included. If we can neglect water drainage through the shell, the dependence of force on relative deformation (for $r_s \gg r_0$ and $\nu = {}^1/_2$) is given by[6]

$$\mathcal{F} \sim \frac{\pi}{2\sqrt{2}} E h^2 \epsilon^{1/2} + 4\pi E h r_0 \epsilon^3 \qquad (1)$$

where E is Young's modulus of the multilayer and h is its thickness. The value of h can be calculated as a product of the number of PSS/PAH bilayers in the shell and the thickness of one bilayer. The values reported for bilayer thickness vary in the range ≈3−5 nm[22,24] and were reported to be independent of molecular weight.[8] Here we use the average value of 4 nm. The data for $\mathcal{N}$ capsules at $\epsilon \leq 0.1$ are well fitted with $E = 200$ MPa. The fit for $\mathcal{N}$ capsules is quite good, except for very small deformations $\epsilon \leq 0.02$, which is partly due to inevitable noncoaxiality of the sphere−capsule interaction, and some (over)simplifications introduced in the derivation of the first, bending, term in eq 1, which dominates at $\epsilon \rightarrow 0$.[2,6] There is an obvious discrepancy between the data for A capsules and the theoretical curve calculated with eq 1. An alternative model, which assumes a rapid (compared to the time scale of the AFM compression experiment) drainage of the inner solution, can be obtained if we simply omit the second, stretching, term in the model of impermeable capsules[10]

$$\mathcal{F} \sim \frac{\pi}{2\sqrt{2}} E h^2 \epsilon^{1/2} \qquad (2)$$

A theoretical curve calculated using Young's modulus, $E = 200$ MPa, found for $\mathcal{N}$ capsules is included in Figure 4. The data set for $\mathcal{A}$ capsules is confined between the predictions of eqs 1 and 2. Of course, this immediately raises a difficulty: the simple models that we have used here assume either zero or infinite permeability of the compressed capsule shells, so that for $\mathcal{A}$ capsules they can only be considered as a first approximation. Nevertheless, the estimates presented here demonstrate the effect of permeability in the softening and aging of the capsules. A full calculation of force vs deformation profiles with finite permeability of the multilayer shell remains very difficult and well beyond the scope of this paper.

One possible explanation for a more rapid drainage of water from $\mathcal{A}$ compared to $\mathcal{N}$ capsules can be obtained if we invoke the increase in size and/or number of nanopores of the multilayer shell, so we have performed a simple permeability test. The $\mathcal{A}$ and $\mathcal{N}$ capsules were exposed to dye (FITC-dextran) solution for 24 h, and then, after thorough rinsing with water, the intensity of fluorescence from the capsule interior was measured. Typical confocal images of the capsules are presented in Figure 5. Since the intensity of fluorescent signal is proportional to the concentration of FITC-dextran, one can conclude that the $\mathcal{A}$ capsules are nearly impermeable to FITC-dextran molecules. In contrast, the $\mathcal{N}$ capsules contains FITC-dextran in the interior. The highest concentration of encapsulated FITC-dextran was observed for FITC-dextran of $M_w \sim 70$ kDa. It was previously suggested that the permeability of the multilayer shell for macromolecules correlates with the nanopore structure.[25,26] Therefore, most likely our result reflects the size of nanopores. One can speculate that the nanopores of the $\mathcal{N}$ capsules are large enough to allow fast release of FITC-dextran of $M_w \sim 4$ kDa during rinsing and measurements. They could be, however, rather small to allow encapsulation of FITC-dextran of $M_w \sim 150$ kDa. Thus, our permeability test suggests that some accidental defects occurring during the capsule preparation (template dissolution) disappear with time. In other words, it indicates that the multilayer shells tend to show a kind of a self-healing capacity. The notion of self-healing was suggested before for supported multilayers[9] and normally indicates the capacity to build smooth defect-free multilayers despite imperfections typically found after adsorption of the first layer. Here for the first time we observe another

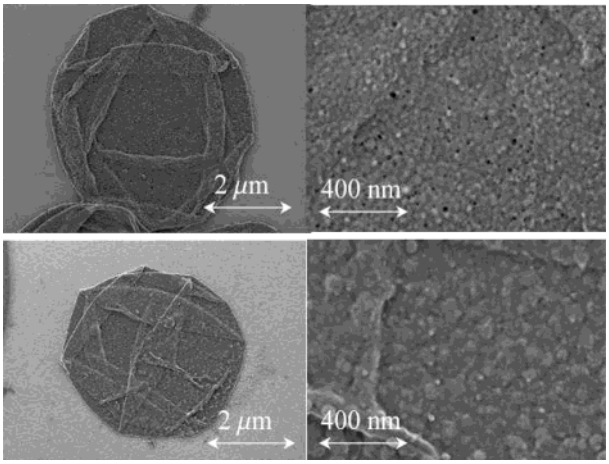

Figure 6. SEM images of $\mathcal{N}$ (top) and $\mathcal{A}$ (bottom) capsules

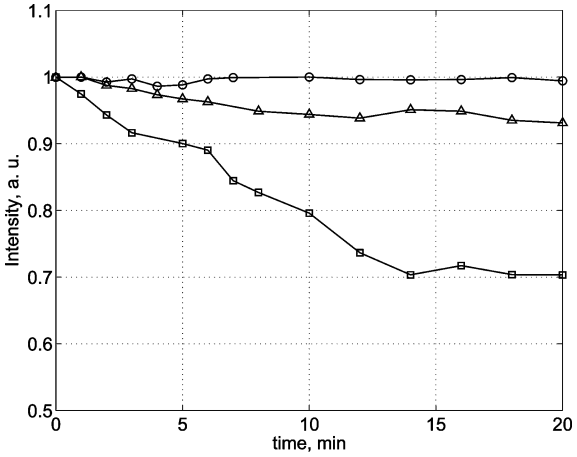

Figure 7. Intensity of fluorescence from the interior of compressed $\mathcal{N}$ capsules filled with low molecular weight rhodamine solution ($\sim 10^{-5}$ mol/L). From top to bottom $\epsilon = 0.1$, 0.2, and 0.5.

recovery process, which we call time self-healing, of the free-standing multilayers forming the capsule shells.

Since the permeability test represents indirect evidence of nanopore structures of multilayer films in water, we have also made and analyzed SEM images of dried $\mathcal{A}$ and $\mathcal{N}$ capsules (see Figure 6). It is seen that both collapse upon drying by forming structures with folds and creases. The morphology of the surfaces of dried $\mathcal{A}$ and $\mathcal{N}$ capsules seems to be indeed very different. SEM images of the surfaces of $\mathcal{N}$ capsules clearly show some nanopores of diameter 2−20 nm, while the images of $\mathcal{A}$ capsules do not reveal any nanopore structure. This result strongly supports the above hypothesis of time self-healing.

Of course, the presence of nanopores in the dried and collapsed state does not necessarily mean that $\mathcal{N}$ capsules in water had them, too. However, both the absence of nanopores in the $\mathcal{A}$ capsules dried under exactly the same conditions, and the correlation with the permeability test in water indicates that they are not created just by drying or at high vacuum. There is, therefore, a good chance that the nanopores in the dried state of freshly prepared capsules reflect their size and existence in water.

To our knowledge, these results represent the first direct observation of small nanopores in a shell of multilayer microcapsules. Despite several attempts, nanopores of this size have not been observed in previous research. The point is that that such nanopores are too small to be detected with the experimental technique applied before.[25,27] Indeed, previous SEM analysis of the shell structures[27] used a standard preparation procedure for SEM, which includes coating of the sample surfaces with a gold layer to avoid charging when using higher acceleration voltage. This additional gold layer may smear topographical structures smaller than 40 nm or even cover them. Hence, most likely it is impossible to observe the small nanopores after gold sputtering. Indeed, the only SEM report on nanopores in multilayer films concerns supported multilayers and larger (20−50 nm) nanopores induced by low pH.[28] It is also clear that the nanopores we observed here in the shell of $\mathcal{N}$ capsules are smaller than the diameter of an AFM tip, which is why they were not detected with AFM imaging, although again, the presence of larger nanopores (100 nm) in dried and collapsed capsules treated in acidic solutions has been reported.[25]

Thus, both the permeability test and SEM analysis suggested that the nanopore/defect structure of the multilayers is characteristic of $\mathcal{N}$ capsules but tends to disappear with time and is not typical for $\mathcal{A}$ capsules. This indicates that the faster drainage from the $\mathcal{A}$ capsule interior in the AFM compression experiment has no direct correlation with the nanopore structure of the multilayer (which, however, seem to control the diffusion through the undeformed shell). One can speculate that despite time self-healing the $\mathcal{A}$ capsules reveal some fragility. In that case, the AFM compression could easily cause rupture of the shell and formation of larger defects. This hypothesis is indirectly confirmed by some steps/discontinuities in the force curves measured for $\mathcal{A}$ capsules even at small relative deformations (Figure 4). It is also consistent with the SEM images (Figure 6), which show many more folds with sharper edges in the case of $\mathcal{A}$ capsules. Clearly, more work is needed to confirm this (fragility) hypothesis and further understand why permeability under compression (drainage) differs from that for undeformed capsules (diffusion). One can, however, suggest that the presence of small nanopores in the shell of $\mathcal{N}$ capsules cannot influence/accelerate drainage of the inner solution at relatively small ϵ, especially on the time scale of the AFM compression experiment. Indeed, as a rough estimate one can assume that flow through the shell

$$\mathcal{Q} \propto N \frac{\pi \rho^4 \Delta P}{8 \mu h}$$

where N is the number of nanopores, ρ is their radius, μ is the dynamic viscosity of water, and ΔP is the excess pressure inside the capsule. The latter can be estimated as a force divided by area of a contact, which for $\epsilon \sim 0.1$ would be approximately $\mathcal{F}(2\pi r_0^2 \epsilon) \sim 10^3$ Pa. It follows from Figure 6 that the area 400 × 400 nm^2 contains about 10 nanopores, so that for a capsule of $r_0 = 2$ μm the number of nanopores $N \sim \pi \times 10^2$. From here with our experimental parameters, and assuming $\rho = 5$ nm, we get $\mathcal{Q} \sim 10^{-19}$ m^3/s. Since with our driving speeds it takes 0.02−0.2 s to reach $\epsilon \sim 0.1$, the loss of volume due to drainage can be estimated as $\Delta V \sim 10^{-21}$−10^{-20} m^3, which is at least 10^3 times smaller than the initial volume of the capsule. Clearly, such a decrease of volume is negligibly small. In fact, the flow rate through the shell is even smaller, since the drainage of the inner

solution would effectively reduce ΔP. Beside that, in general there could be more nanopores in the dried state than in the wet state, but never the opposite. So, our approach can only overestimate flow rate.

We leave the matter by presenting the results of another simple permeability test, which demonstrates this. Figure 7 shows the decrease in intensity of fluorescence with time inside compressed $\mathcal{N}$capsules filled with rhodamine (encapsulation took 4 days). One can see that no drainage is detected at $\epsilon = 0.1$, but drainage is getting significant at larger relative deformations, when, according to our force experiment, we deal with the formation of large pores in the shell and/or its rupture.

IV. Final Remarks

Certain aspects of our work warrant further comments.

First, we have found that mechanical properties of multilayer microcapsules do not depend on the molecular weight of shell-forming polyelectrolytes. This conclusion both agrees and disagrees with the observations of different authors. Namely, our results are consistent with the previous structure studies[8,9,14,15] but are different from the recent mechanical experiment.[13] The reasons for disagreement are not entirely clear. One might be hidden in the assumptions of the model[13] used to fit experimental data (see refs 2, 3, and 6 for more details). Another might be due to the use of relatively low molecular weight PAH (average $M_w \sim 10$ kDa) in one of two samples studied in ref 13. For such short chains one cannot exclude some reversibility in the polyelectrolyte adsorption and, therefore, some loss of polymer.[15,17,29] If so, the weak softening of such capsules might be due to a decrease in the shell thickness but not in Young's modulus of the multilayer.

Second, we have detected softening of the multilayer microcapsules over a relatively large time scale. We have shown that the aged capsules get softer due to the faster drainage of the inner solution under compression and suggested that this is due to enhanced fragility (or a decrease in the rupture strength) of the aged capsules compared with the freshly prepared ones. To the best of our knowledge, these issues were never addressed before. This completely neglected effect of aging is poorly understood at the moment and has to be studied in more detail.

Third, we have obtained results that may add a new dimension to the problem of permeability of polyelectrolyte multilayers. Our experiment suggested that there exist in the multilayer shells of freshly prepared microcapsules tiny defects/pores. Their size appears to be of the order of a few nanometers. This nanopore structure disappears within a few months, which suggested a new concept of a time self-healing. It is probable that these small nanopores are responsible for higher permeability of newly prepared and undeformed capsules for small and even for polymer molecules, although we do not, and still cannot, claim universality. An entirely unexpected observation is that this diffusion permeability does not correlate with the speed of drainage through the shell of compressed capsules. The drainage permeability seems to depend mostly on the existence of larger pores induced by the stretching/rupture of the shells of the compressed capsules. Clearly, to understand better some variability and certain contradictions in the results of different groups concerning permeability and mechanical properties of the shells,[6,10,13,25,30] all these results should be taken into account.

Acknowledgment. We thank B. S. Kim, O. V. Lebedeva, and I. Lieberwirth for helpful discussions and G. Glasser for making SEM images.

References and Notes

(1) Donath, E.; Sukhorukov, G. B.; Caruso, F.; Davis, S. A.; Möhwald, H. *Angew. Chem., Int. Ed.* **1998**, *37*, 2202.
(2) Vinogradova, O. I. *J. Phys.: Condens. Matter* **2004**, *16*, R1105.
(3) Vinogradova, O. I.; Andrienko, D.; Lulevich, V. V.; Nordschild, S.; Sukhorukov, G. B. *Macromolecules* **2004**, *37*, 1113.
(4) Lulevich, V. V.; Radtchenko, I. L.; Sukhorukov, G. B.; Vinogradova, O. I. *J. Phys. Chem. B* **2003**, *107*, 2735.
(5) Lulevich, V. V.; Radtchenko, I. L.; Sukhorukov, G. B.; Vinogradova, O. I. *Macromolecules* **2003**, *36*, 2832.
(6) Lulevich, V. V.; Andrienko, D.; Vinogradova, O. I. *J. Chem. Phys.* **2004**, *120*, 3822.
(7) Shackelford, J. F.; William, A.; Juns, P. *Material Science and Engineering Handbook*; CRC Press: Boca Raton, FL, 1992.
(8) Lösche, M.; Schmitt, J.; Decher, G.; Bouwman, W. G.; Kjaer, K. *Macromolecules* **1998**, *31*, 8893.
(9) Bertrand, P.; Jonas, A.; Laschewsky, A.; Legras, R. *Macromol. Rapid Commun.* **2000**, *21*, 319.
(10) Lulevich, V. V.; Vinogradova, O. I. *Langmuir* **2004**, *20*, 2874.
(11) Kim, B. S.; Vinogradova, O. I. *J. Phys. Chem. B* **2004**, *108*, 8161.
(12) Hoogeven, N. G.; Cohen Stuart, M. A.; Fleer, G. J. *Langmuir* **1996**, *12*, 3675.
(13) Gao, C.; Donath, E.; Moya, S.; Dudnik, V.; Möhwald, H. *Eur. Phys. J. E* **2001**, *5*, 21.
(14) Kolarik, L.; Furlong, D. N.; Joy, H.; Struijk, C.; Rowe, R. *Langmuir* **1999**, *15*, 8265.
(15) Sui, Z.; Salloum, D.; Schlenoff, J. B. *Langmuir* **2003**, *19*, 2491.
(16) Cheung, J. H.; Stockton, W. B.; Rubner, M. F. *Macromolecules* **1997**, *30*, 2712.
(17) Dubas, S. T.; Schlenoff, J. B. *Macromolecules* **2001**, *34*, 3736.
(18) McAloney, R. A.; Goh, M. C. *J. Phys. Chem. B* **1999**, *103*, 10729.
(19) Casson, J. L.; Wang, H. L.; Roberts, J. B.; Parikh, A. N.; Robinson, J. M.; Johal, M. S. *J. Phys. Chem. B* **2002**, *106*, 1697.
(20) Koetse, M.; Laschewsky, A.; Jonas, A. M.; Verbiest, T. *Colloids Surf. A* **2002**, *198−200*, 275.
(21) Kim, J.; Kim, G.; Cremer, P. S. *J. Am. Chem. Soc.* **2002**, *124*, 8751.
(22) Sukhorukov, G. B.; Donath, E.; Lichtenfeld, H.; Knippel, E.; Knippel, M.; Budde, A.; Möhwald, H. *Colloids Surf. A* **1998**, *137*, 253.
(23) Dähne, L.; Leporatti, S.; Donath, E.; Möhwald, H. *J. Am. Chem. Soc.* **2001**, *123*, 5431.
(24) Sukhorukov, G. B.; Donath, E.; Davis, S.; Lichtenfeld, H.; Caruso, F.; Popov, V. I.; Möhwald, H. *Polym. Adv. Technol.* **1998**, *9*, 759.
(25) Antipov, A. A.; Sukhorukov, G. B.; Leporatti, S.; Radtchenko, I. L.; Donath, E.; Möhwald, H. *Colloids Surf. A* **2002**, *198−200*, 535.
(26) Lvov, Y.; Antipov, A. A.; Mamedov, A.; Möhwald, H.; Sukhorukov, G. B. *Nano Lett.* **2001**, *1*, 125.
(27) Sukhorukov, G. B.; Shchukin, D. G.; Dong, W. F.; Möhwald, H.; Lulevich, V. V.; Vinogradova, O. I. *Macromol. Chem. Phys.* **2004**, *205*, 530.
(28) Mendelsohn, J. D.; Barret, C. J.; Chan, V. V.; Pal, A. J.; Mayer, A. M.; Rubner, M. F. *Langmuir* **2000**, *16*, 5017.
(29) Schlenoff, J. B.; Ly, H.; Li, M. *J. Am. Chem. Soc.* **1998**, *120*, 7626.
(30) Ibarz, G.; Dähne, L.; Donath, E.; Möhwald, H. *Adv. Mater.* **2001**, *13*, 1324.

MA049140+